Effect of Shape Deformation by Edge Roughness in Spin-Orbit Torque Magnetoresistive Random-Access Memory

Jihun Byun, Doo Hyung Kang, and Mincheol Shin*
School of Electrical Engineering
Korea Advanced Institute of Science and Technology
Daejeon 34141, Republic of Korea
*mshin@kaist.ac.kr

***Abstract*— We present a micromagnetic simulation study of shape deformation and edge roughness effect in the spin orbit torque-magnetic random access memory (SOT-MRAM). The two different write schemes, magnetic field induced SOT write scheme and SOT-spin transfer torque (STT) hybrid write scheme, were studied in the presence of the stray field from the reference layer. We found that for conventional magnetic field induced SOT, shape deformation can cause non-deterministic switching even at a relatively high gilbert damping constant of 0.08. Higher Gilbert damping constant (α) of 0.09 is needed to ensure deterministic switching under the shape deformation effect. The SOT-STT hybrid write scheme showed deterministic switching even at lower damping constant with relatively low device variations due to the constant –z directed torque of the STT. However, with higher damping constant of α = 0.1, device variation with the SOT-STT hybrid write scheme increases while the SOT-magnetic field write scheme successfully compensates the most of the variation caused by the edge deformation.**

Keywords—Magnetic Random Access Memory, Spin Orbit Torque, Spin Transfer Torque, Damping constant, Micromagnetic simulation

I. INTRODUCTION

Spin-orbit torque magnetoresistive random-access memory (SOT-MRAM) is a promising novel non-volatile memory device due to sub-ns operation speed and higher reliability compare to spin-transfer torque magnetoresistive random-access memory (STT-MRAM). Writing operation involves the current flowing through the heavy metal beneath the magnetic tunnel junction (MTJ). This current induces in-plane torque driven by spin Hall effect (SHE) and/or Rashba effect. Unlike STT, of which the direction is perpendicular, SOT has the in-plane directed torque therefore it only lays down the initially perpendicular magnetization (z-direction) towards the spin-polarized direction in the x-y plane. Additional torque is required to complete the switching. For this purpose, one of the most commonly used methods is to apply the in-plane magnetic field. The in-plane field would tilt the magnetization towards the targeted hemisphere and relax towards the targeted state upon turning off the SOT current. Although it required an external magnetic field, newly proposed methods suggest that the external field-free SOT-MRAM is possible by imposing a magnetic hard mask [1] or using antiferromagnet/ferromagnet bilayer [2] or ferromagnet/heavy metal/ferromagnet trilayer [3]. This write scheme using the in-plane magnetic field will be referred as the SOT-magnetic field write scheme in the rest of the paper for simplicity. Another well-known write scheme is the SOT-STT hybrid write scheme, which uses STT current to induce perpendicular torque instead of the magnetic field [4]. It requires additional STT current but it tends to have a simpler MRAM structure as there is no need for additional process to provide the effective in-plane magnetic field. Both write schemes demonstrated sub-ns switching with lower writing power compared with the MRAM using the STT write scheme alone [1, 4]. Despite the outstanding performance of the SOT-MRAM, it lacks the study of the expected variation in the switching characteristics as the SOT-MRAM has not been yet commercially mass-produced.

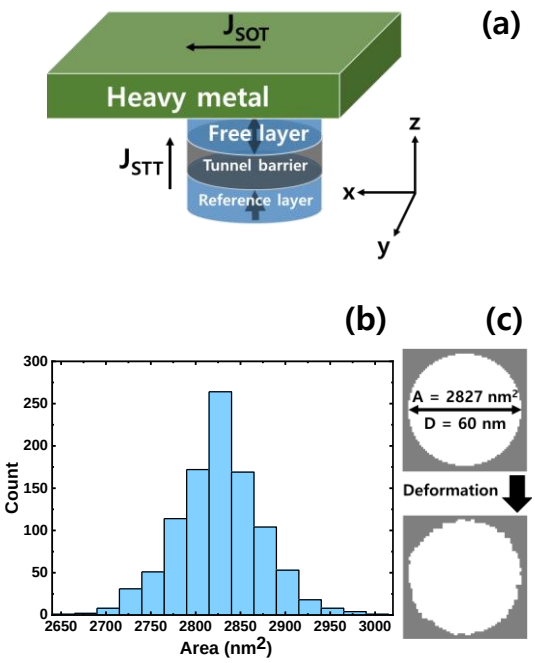

Fig. 1. (a) Typical structure of SOT-MRAM and (b) the distribution of the area of the generated MTJ samples and (c) deformation process

The magnetization reversal process can be affected by boundary roughness [5] and the shape deformation of MTJ has an influence on switching time in STT-MRAM due to the in-plane demagnetizing tensor induced from deformed MTJ [6]. The MTJs have suffered from critical dimension variations during the manufacturing process [7] and fabricated MTJs indicate that they are not in perfect circular shape [8]. The shape deformation of MTJ is expected to affect the magnetization switching behavior of the SOT-MRAM but this is not yet elucidated to the best our knowledge. Earlier studies analyzed shape deformation of SOT-MRAM modeled the

TABLE I. PARAMETERS USED IN THE SIMULATION

Symbol	Parameters	Value
A	Damping constant	0.02 ~ 0.1
θ_{SH}	Spin hall angle	0.3
H	Spin torque efficiency	0.7
$Ku1_{free}$	Anisotropy constant of the free layer	9.8×10^{5} J/m^3
$Ku1_{reference}$	Anisotropy constant of the reference layer	1.5×10^{6} J/m^3
A_{ex}	Exchange constant	20×10^{-12} A/m
M_{sat}	Saturation magnetization	1.2×10^{6} A/m
t_F	Free layer thickness	1 nm
t_R	Reference layer thickness	1 nm
t_T	Tunnel barrier thickness	1 nm
D	MTJ Diameter	60 nm
	Mesh size	$1\times 1\times 1$ nm^3
T_{SOT}	SOT pulse width	1 ns
T_{STT}	STT pulse width	5 ns

shape deformation by varying the area of the MTJ rather than considering altered edge and shape of MTJ [9].

In this work, we present a micromagnetic simulation study of shape deformation due to edge roughness effect in the SOT-MRAM. Two different writing schemes of SOT-MRAM were studied; the SOT-magnetic field write scheme and the SOT-STT hybrid write scheme.

II. METHODOLOGY

To consider the shape deformation, micromagnetic simulations were performed by using object oriented micromagnetic framework (OOMMF) [10]. Simulated SOT-MRAM has a structure shown in Fig. 1. Ideal MTJ's are of the cylindrical shape and consist of three layers of free layer, tunnel barrier, and reference layer, each of which has a thickness of 1 nm and diameter of 60 nm. We assumed that the heavy metal on the top of the free layer provides SOT current with the spin polarization ($\vec{\sigma}$) along the –y-direction. Perpendicularly (z-direction) magnetized MRAM was considered with the initial free layer and the reference layer magnetization in +z-direction. We treated 1000 samples each with x-y plane random edge roughness on ideal circular-shaped MTJ to have ±5% of area difference within 3σ distributions. Field-like torque induced by STT and SOT was not considered in this simulation.

The SOT-magnetic field write scheme needs SOT current pulse under external magnetic field in x-direction (H_x) and the SOT-STT hybrid write scheme uses both SOT current (J_{SOT}) and STT current (J_{STT}) in the absence of magnetic field. Parameters used in the simulations are shown in Table. 1. H_x of 30 mT was applied for the SOT-magnetic field write scheme case. As can be seen in Fig. 2., the SOT critical current

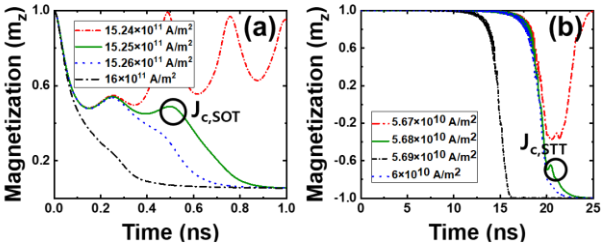

Fig. 2. Critical current of the ideal circular device with the α = 0.02. (a) SOT critical current ($J_{c,SOT}$) and (b) STT critical current ($J_{c,STT}$)

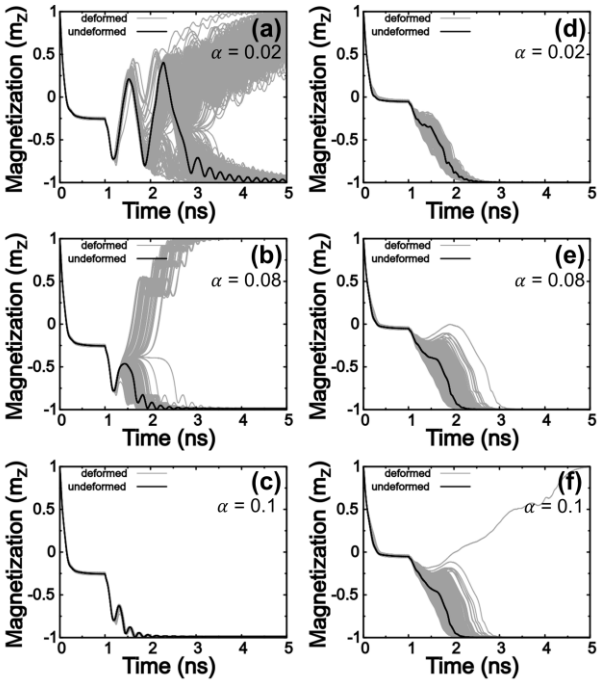

Fig. 3. Time evolution of perpendicular component of the free layer magnetization m_z of SOT-magnetic field write scheme with J_{SOT} = 16×10^{11} A/m^2, H_x = 30 mT, t_{SOT} = 1 ns with damping constant (a) α = 0.02, (b) α = 0.08, and (c) α = 0.1. SOT-STT hybrid write scheme with J_{SOT} = 16×10^{11} A/m^2, J_{STT} = 6×10^{10}, t_{SOT} = 1 ns, t_{STT} = 5 ns with damping constant (d) α = 0.02, (e) α = 0.08, and (f) α = 0.1. Bold and gray lines represent the circular MTJ without deformation and the deformed samples with random edge roughness, respectively.

($J_{c,SOT}$) was 15.25×10^{11} A/m^2 and STT critical current ($J_{c,STT}$) was 5.68×10^{10} A/m^2. Therefore, the operation currents were chosen to have a higher value than the critical current to ensure switching, which were J_{SOT} = 16×10^{11} A/m^2 and J_{STT} = 6×10^{10} A/m^2. Square current pulse was assumed.

III. RESULTS AND DISCUSSION

Fig. 3 represents the z-direction component of the magnetization (m_z) under the SOT-magnetic field write scheme when the Gilbert damping constants (α) were 0.02, 0.08, and 0.1. As shown in Fig. 3. (a), only 42.3% of samples are switched for the SOT-magnetic field write scheme with low α of 0.02 and the ideal circular MTJ shows a highly oscillatory magnetization trajectory. At α as high as 0.08, the sample without the deformation shows stable damping with precession which occurs only in the lower hemisphere. However, α is not high enough that the switching probability of 100% was still not achievable (see Fig. 3 (b)).

The relatively low α induces unstable magnetization trajectory with the high precession amplitude which crosses to the upper hemisphere (m_z > 0) and damps toward the stable initial state. The earlier work explains such unstable switching as the hysteric behavior of the transition to the intermediate position, where the behavior intensifies with the lower α [11]. Such an unstable magnetization trajectory makes the switching sensitive to various field terms, that demagnetization field alternation due to ±5% deformation in the area within 3σ is enough to cause more than half of the samples to switch back to the initial state.

Another possible influence from the shape deformation is the edge roughness affecting the nucleation and the

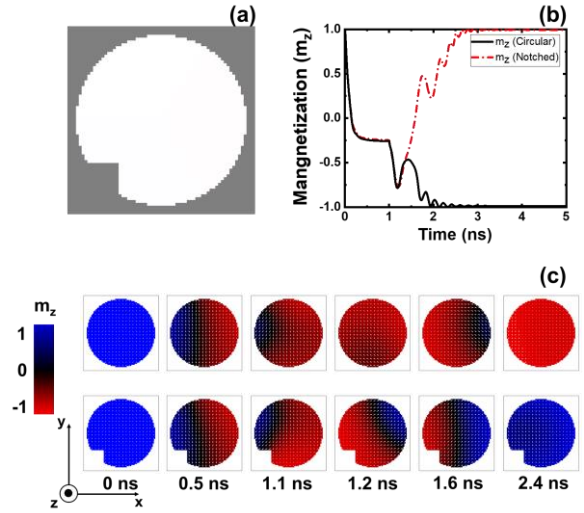

Fig. 4. (a) sample with 10 nm × 10 nm edge notch (b) Time evolution of perpendicular component of the free layer magnetization m_z of SOT-magnetic field write scheme with α = 0.08, compared with the ideal circular MTJ. (c) magnetization snapshots of the free layer. Blue inditcates the parallel state, red indicates the antiparallel state and black indicates the in-plane magnetization. Top line is the snapshots of the circular MTJ and the Bottom line is the snapshots of the edge notched MTJ.

propagation of the domain. Fig. 4. (b) depicts the magnetization trajectory of the edge notched MTJ and the ideal circular MTJ using the SOT-magnetic field write scheme with α = 0.08. From Fig. 4. (c), it can be seen that the switching behavior of the MTJs involves asymmetric nucleation of the edge and the propagation. Such behavior is known to be seen in the presence of the Dzyaloshinskii-Moriya interaction (DMI) causing the inward or outward magnetization canting of the edge [12]. We estimate that the asymmetric edge nucleation and propagation were derived by the stray field. This is because the reference layer can induce a similar effect as the edge canting of the DMI due to the inward or outward in-plane stray magnetic field at the edge [13, 14].

With the edge notch, the propagation characteristics can be altered from the ideal case as the propagation of the domain is disturbed by the notch therefore fails to completely propagate to the opposite end. The magnetic domain nucleation and propagation can be largely affected by the edge roughness [5] and we estimate that they are the origin of the switching characteristics variations and switch failure derived from the edge roughness.

As shown in Fig. 3. (c), 100% switching is possible for a higher α of 0.1. Also, using α of 0.1 results in lower device variations of maximum switching time difference of 3.57% with the average switching time of 1.42 ns. Those for the α = 0.02 are 87.74% and 3.14 ns, respectively. This is because the higher α induces less oscillatory magnetization so that the precession only occurs in the lower hemisphere (m_z < 0) and does not cross the equator (m_z = 0). Higher α induces higher –z directed effective magnetic field in the –z-direction magnetized domain region due to the perpendicular anisotropy. Since the domain is larger in size after the SOT pulse is turned off, higher α will more favor this domain to propagate towards the +z-direction magnetized domain region side. However, the widely used MTJ structure of the CoFeB/MgO layer has α of 0.01 ~ 0.03 [15]. Within these values, one cannot achieve deterministic switching

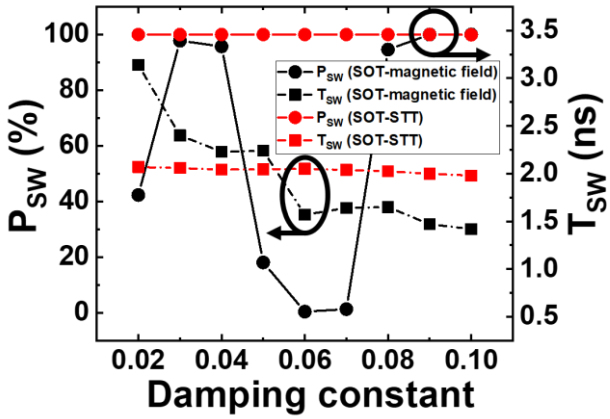

Fig. 5. Switching probability (P_{SW}) and switching time (T_{SW}) with damping constant α variation. Red lines indicate the SOT-STT hybrid write scheme and black lines indicate the SOT-magnetic field write scheme.

independent of shape deformation caused by process variations.

Fig. 3. (d) shows the results of the SOT-STT hybrid write scheme at α = 0.02. The SOT-STT hybrid write scheme enables the switching of all samples even at relatively low α. This is because the perpendicular ($-\mathbf{m}\times(\mathbf{m}\times\hat{\boldsymbol{z}})$) torque of the STT suppresses the precession towards the upper hemisphere and induces less oscillatory behavior of magnetization. Less switching time variation of 27.3% and lower switching time of average 2.06 ns were achieved. The SOT-magnetic field write scheme with the same α have an average switching time of 3.14 ns. Also, the switching speed of the SOT-STT hybrid write scheme is 7.63 times faster than the STT write scheme in the absence of the SOT current, which has 15.81 ns of switching time as can be seen in Fig. 2.(b).

The switching trajectory variation in the SOT-STT hybrid write scheme induced by the deformation might be due to the altered in-plane demagnetization tensor, which affects the switching time [6] and the edge roughness, which can slow down the domain propagation [5].

Using the SOT-STT hybrid write scheme, with increasing the α, the device variation increases with almost constant switching time. Also, switching probability degrades to 99.9% when α = 0.1. We analyzed that this is because the intermediate state of the SOT-STT hybrid write scheme has close proximity to the x-y plane. The m_z of the SOT-STT hybrid write scheme at the 1 ns, which is the end of the intermediate state, is only –0.05. Due to this magnetization lying near the equator, after the J_{SOT} is turned off, both parallel (m_z = 1) and the antiparallel (m_z = –1) states of the SOT-STT hybrid write scheme are highly stable. The magnetization switching is also affected by the out-of-plane component of the stray field generated from the reference layer. Therefore, after t = 1 ns, STT in the absence of the SOT has to compete against the damping towards the initial parallel state and the stray field. This hindrance of the switching enlarges with increasing the α, resulting in higher variation. They lead to the degradation of switching characteristics and switching back behavior in α = 0.1.

However, for the SOT-magnetic field write scheme, when t = 1 ns, the intermediate state is located at m_z = –0.26. In this state, the antiparallel state is clearly more stable and the

magnetization can damps towards the targeted state with faster switching time when using higher α.

These tendencies can be seen in Fig. 5 which shows switching probability (P_{SW}) and switching time (T_{SW}) varying with the damping constant α. The T_{SW} of the SOT-magnetic field write scheme decrease with the increasing α, so that its switching probability reaches to 100% at α = 0.09, while the SOT-STT hybrid write scheme switching time is almost independent on α. The oscillatory behavior in P_{SW} of the SOT-magnetic field at lower α agrees with the earlier macrospin work [16].

One might argue that decreasing the in-plane field and increasing J_{STT} can result in better performance of the SOT-STT hybrid write scheme at high α. Note that the $J_{STT} = 6\times10^{10}$ A/m^2 used in the simulation shows the switching time of 15.81 ns which satisfies the target write speed for STT-MRAM used in an L4 cache application of sub 20 ns [17]. While the H_x = 30 mT is also commonly used value for the in-plane magnetic field in the SOT-MRAM [1, 18]. Therefore, the tendency shown in Fig. 5 shows the results using a common magnitude of H_x and J_{STT} rather than the exceptional case.

IV. Consclusion

The performance effect of shape deformation on SOT-MRAM with two different write schemes has been studied by using micromagnetic simulation. It is found that the edge roughness and deformation of MTJ in SOT-MRAM can result in severe variation in switching behavior such as write failure or switching time degradation. The source of the variation might be the alteration of demagnetization tensor and the disturbance in the domain propagation by the rough edge.

The simulation results show that the SOT-magnetic field write scheme may not be practical up to high α of 0.09 because of the low switching probability. The SOT-STT hybrid write scheme shows 100% switching even with α of 0.02, having faster switching and lower device variation compared to the SOT-magnetic field write scheme. However, with the stray field from the reference layer, using high α the SOT-magnetic field write scheme shows better performance with less device variation and enhanced switching speed whereas it results in the degradation of the SOT-STT hybrid write scheme with higher device variation with write failure occurs. A reason for the failure is that the SOT-STT hybrid write scheme has its intermediate state located near the x-y plane. Higher α induces damping towards both parallel and anti-parallel state and the out-of-plane component of the stray field results as the disturbance of the intended switching.

Our results suggest that in the presence of the stray field, the SOT-magnetic field write scheme shows better performance for MTJ with high α whereas the SOT-STT hybrid write scheme shows better performance with low α material.

Acknowledgment

This work was supported by Samsung Research Funding & Incubation Center of Samsung Electronics under Project Number SRFC-IT1901-11

References

[1] K. Garello *et al*., "Magnufacturable 300mm platform solution for Field-Free Switching SOT-MRAM," in 2019 Symposium on VLSI Circuits, Kyoto, Japn, 2019

[2] Y. Oh *et al*., "Field-free switching of perpendicular magnetization through spin-orbit torque in antiferromagnet/ferromagnet/oxide structures," Nat. Nanotech, vol. 11, 878-884, 2016

[3] W. Chen, L. Quain, and G. Xiao, "Deterministic Current Induced Magnetic Switching Without External Field using Giant Spin Hall Effect of β-W," Nat. Sci. Rep., vol. 8, 8144, 2018

[4] S. Pathak, C. Youm, and J. Hong, "Impact of Spin-Orbit Torque on Spin-Transfer Torque Switching in Magnetic Tunnel Junctions," Nat. Sci. Rep., 10, 2799, 2020

[5] D. Meyners, H. Bruckl, and G. Reiss, "Influence of boundary roughness on the magnetization reversal in submicron sized magnetic tunnel junctions," J. Appl. Phys., vol. 93, 2676, 2003.

[6] C. Engel, S. Goolaup, H. Teoh, and W. Lew, "Effect of Geometrical Modulation on pMTJ Magnetization Reversal," IEEE Trans. Magn., vol. 53, no.12, 2017.

[7] K. Lee *et al.*, "1Gbit High Density Embedded STT-MRAM in 28nm FDSOI Technology," in 2019 IEEE International Electron Devices Meeting (IEDM), San Francisco, CA, USA, 2019.

[8] M. Pak *et al.*, "LCDU optimization of STT-MRAM 50nm pitch MTJ pillars for process window improvement," in Proc. Extreme Ultraviolet (EUV) Lithography X, San Jose, CA, USA, 2019.

[9] B. Zeinali, J. Madsen, P. Raghaan, and F. Moradi., "Ultra-Fast SOT-MRAM Cell with STT Current for Deterministic Switching," in 2017 IEEE International Conference on Computer Design (ICCD), Boston, MA, USA, 2017.

[10] R. McMichael and M. Donahue, "OOMMF User's Guide, Version 1.0," National Institute of Standards and Technology, Gaithersburg, MD, USA, Interagency Report NISTIR 6376, Sept. 1999.

[11] B. chen, S. Lim, and M. Tran, "Magnetization Switching of a Thin Ferromagnetic Layer by Spin-Orbit Torques," IEEE Magn. Lett., vol. 7, 2016

[12] N. Mikuszeit, *et al.*, "Spin-orbit torque driven chiral magnetization reversal in ultrathin nanostructures," Phys. Rev. B., Vol.2, 14424, 2015

[13] Y. Wang, *et al.*, "Impact of the stray field on the switching properties of perpendicular MTJ for scaled MRAM," in 2012 IEEE International Electron Devices Meeting (IEDM), San Francisco, CA, USA, 2012.

[14] H. Jiancheng, *et al.*, "Effect of the stray field profile on the switching characteristics of the free layer in a perpendicular magnetic tunnel junction," J. Appl. Phys., vol. 117, 17B721, 2015

[15] S. Ikeda, *et al*., "A Perpendicular-anisotropy CoFeB-MgO magnetic tunnel junction," Nat. Mat., 9, 721-724, 2010

[16] K. Lee, S. Lee, B. Min, and K. Lee, "Threshold current for switching of a perpendicular magnetic layer by spin Hall effct," Appl. Phys. Lett., vol. 102, 112410, 2013

[17] J.G. Alzate, *et al.*, "2 MB Array-Level Demonstration of STT-MRAM Process and Performance Towards L4 Cache Applications," in 2019 IEEE International Electron Devices Meeting (IEDM), San Francisco, CA, USA, 2019.

[18] N. Sato, F. Xue, R. M. White, C. Bi, and S. X. Wang, "Two-terminal spin–orbit torque magnetoresistive random access memory", Nat. Electron., vol. 1, 508-511, 2018